Impurity effects on the resonant Andreev reflection in a finite-sized carbon nanotube system

Hui Pan, Tsung-Han Lin, and Dapeng Yu

Department of Physics, State Key Laboratory for Mesoscopic Physics,

Peking University, Beijing 100871, P. R. China

Abstract

The influence of the impurity on the resonant Andreev reflection through a normal-metal/carbon-nanotube/superconductor system is studied theoretically. It is found that the resonant Andreev reflection depends on the strength of the impurity and the length of the armchair nanotube. The impurity which breaks the electron-hole symmetry of the nanotubes greatly reduces the resonant Andreev reflection. The symmetry broken depends distinctly on the impurity strength. The impurity effects on the Andreev reflection current at different bias are also studied.

Carbon nanotubes have been the subject of an increasing number of experimental and theoretical studies due to their quasi-one-dimensional structure and unique electronic property.[1] The perfect carbon nanotube is predicted to be either metallic or semiconducting sensitively depending on its diameter and chirality, which is uniquely determined by the chiral vector (n, m), where n and m are integers.[1,2,3,4] Experimental and theoretical studies have indicated that the electronic and transport properties of carbon nanotubes can be substantially modified by point defects such as the substitutional impurities.[5,6,7,8,9,10,11] One of recent interests concentrates on the electron transport through hybrid nanotube system. Experiments about some hybrid systems including nanotube-based magnetic tunnel junctions[12] and superconducting junctions[13,14] have been successfully fabricated. The electrical transport transport about the carbon nanotube quantum dot in the Kondo regime coupled to a normal and a superconductor has also been reported.[15] The theoretical investigation of transport properties of these hybrid nanotube devices is of great importance, not only for their basic scientific interest, but also aiming at the design of novel nanodevices.

The resonant Andreev reflections in the superconductor/carbon-nanotube devices has been theoretically studied.[16] The proximity effect in superconductor/carbon-nanotube/superconductor (S/CNT/S) tunnel junctions has also been studied theoretically.[17] However, the effects of the impurity, such as the substitutional boron (nitrogen) and the vacancy, in these systems are not considered. In this paper, the effects of the substitutional boron (nitrogen) and the vacancy on the resonant Andreev reflection in the hybrid normal-metal/carbon-nanotube/superconductor (N/CNT/S) system are theoretically studied. In such a system, the specific molecular orbital plays an important role. By combing standard nonequilibrium Green's function (NGF) techniques[18,19,20] with a tight-binding model,[21,22] we have analyzed quantum transport properties of the N/CNT/S system with the substitutional boron (nitrogen) and the vacancy. The Andreev reflection through the finite-sized carbon nanotube depends on the impurity strength and the tube length. The substitutional impurity, such as the boron and nitrogen, reduces the resonant Andreev reflection greatly. However, the impurity with very large strength, such as the vacancy, does not reduce the resonant Andreev reflection. The dependence of the Andreev reflection current with the gate voltage is also studied.

We assume that the system N/CNT/S under consideration is described by the following

Hamiltonian:

$$H = H_L + H_R + H_{tube} + H_T, \tag{1}$$

where

$$H_L = \sum_{k,\sigma}(\epsilon^0_{L,k} - ev_L)a^\dagger_{L,k\sigma}a_{L,k\sigma}, \tag{2}$$

$$H_R = \sum_{p,\sigma}\epsilon^0_{R,p}a^\dagger_{R,p\sigma}a_{R,p\sigma} + \sum_p[\Delta^* a^\dagger_{R,p\downarrow}a_{R,-p\uparrow} + \Delta a^\dagger_{R,-p\uparrow}a_{R,p\downarrow}],$$

$$H_{tube} = \sum_{\langle i,j\rangle,\sigma}[\gamma_0 c^\dagger_{i\sigma}c_{j\sigma} + H.c.] - \sum_{i,\sigma}ev_g c^\dagger_{i\sigma}c_{i\sigma} + U c^\dagger_0 c_0,$$

$$H_T = \sum_{k,\sigma,i}[t_L a^\dagger_{L,k\sigma}c_{i\sigma} + H.c.] + \sum_{p,\sigma,i}[t_R e^{iev_R\tau}a^\dagger_{R,p\sigma}c_{i\sigma} + H.c.],$$

where H_L describes the noninteracting electrons in the left normal-metal lead, $a^\dagger_{L,k\sigma}(a_{L,k\sigma})$ are the creation (annihilation) operators of the electron in the left lead, and v_L is the voltage of the left lead. H_R describe the right superconducting lead with the energy gap Δ. The nanotube Hamiltonian H_{tube} is described by the tight-binding model with one π-electron per atom at i site. The sum in i, j is restricted to nearest-neighbor atoms, and the bond potential $\gamma_0 = -2.75eV$, which is used as the energy unit. This model is known to give a reasonable, qualitative description of the electronic and transport properties of carbon nanotubes.[21,22] For simplicity, the intra-tube electron-electron Coulomb interaction has been neglected. v_g is the gate voltage which controls the energy levels in the CNT. The pointlike defect is defined by setting site energy equal to U at one of the sites of the unit cell, and various strengths represent typical substitutional impurities or vacancy.[10]. According to former tight-binding and *ab inito* calculations,[10,11] we set the strength $U = 3, -5$, and 10000 to simulate the substitutional boron, nitrogen and vacancy, respectively. H_T denotes the tunneling part of the Hamiltonian, and $t_{L,R}$ are the hopping matrix. It is convenient to introduce the 2×2 Nambu representation in which the Green's function can be expressed by

$$G^{r,a}(\tau,\tau') = \mp i\theta(\tau \mp \tau')\sum_{ij}\begin{pmatrix} \langle c_{i\uparrow}(\tau), c^\dagger_{j\uparrow}(\tau')\rangle & \langle c_{i\uparrow}(\tau), c_{j\downarrow}(\tau')\rangle \\ \langle c^\dagger_{i\downarrow}(\tau), c^\dagger_{j\uparrow}(\tau')\rangle & \langle c^\dagger_{i\downarrow}(\tau), c_{j\downarrow}(\tau')\rangle \end{pmatrix}, \tag{3}$$

The retarded Green's function of the nanotube is calculated directly using a tight-bingding model via

$$g^r(\epsilon) = \begin{pmatrix} \frac{1}{\epsilon - H_{tube} + i0^+} & 0 \\ 0 & \frac{1}{\epsilon + H_{tube} + i0^+} \end{pmatrix}. \tag{4}$$

Using the standard NGF technique[18,19,20], the Green's functions are obtained as

$$G_{11}^r(\epsilon) = [(g_{11}^r(\epsilon))^{-1} + \frac{i}{2}\Gamma_L + \frac{i|\epsilon|}{2\sqrt{\epsilon^2 - \Delta^2}}\Gamma_R + \frac{\Delta^2}{4(\epsilon^2 - \Delta^2)}A^r(\epsilon)]^{-1}, \tag{5}$$

$$G_{12}^r(\epsilon) = G_{11}^r(\epsilon)\frac{\Delta}{2\sqrt{\epsilon^2 - \Delta^2}}\Gamma_R A^r(\epsilon),$$

$$A^r(\epsilon) = [(g_{22}^r(\epsilon))^{-1} + \frac{i}{2}\Gamma_L + \frac{i|\epsilon|}{2\sqrt{\epsilon^2 - \Delta^2}}\Gamma_R]^{-1}.$$

where $\Gamma_{L,R}$ are the appropriate linewidth functions describing the coupling of the CNT to the respective leads. Here G_{11} and G_{12} are the retarded Green's functions of the CNT, which include the proper self-energy of the leads.[18,19,20] Then the current and probability of the Andreev reflection are given by

$$I_A = \frac{2e}{h} \int d\epsilon [f_L(\epsilon + ev_L) - f_L(\epsilon - ev_L)] T_A(\epsilon), \tag{6}$$

$$T_A(\epsilon) = Tr[\Gamma_L G_{12}^r(\epsilon)\Gamma_L G_{12}^{r\dagger}(\epsilon)], \tag{7}$$

where $f_{L,R}$ denote the Fermi functions of the left and right leads, respectively. Clearly, the conventional tunneling is completely forbidden for $V < \Delta$, and only the Andreev reflection exists. In the following numerical calculations, we discuss in detail the Andreev reflection at zero temperature in the case of $V < \Delta$. We set (1) the temperature $\mathcal{T} = 0$, (2) the voltage of the right lead $v_R = 0$ due to the gauge invariance, and carry out all calculations with $\Delta = 1$, and $\Gamma_L = \Gamma_R = 0.02$ in units of $\hbar = e = 1$.

In the following, the probability T_A and current I_A of Andreev reflection for the N/CNT/S hybrid system are calculated. In Fig. 1, T_A is plotted as a function of the incident electron energy for nanotubes with different lengths. For the comparison, the conductance G of the N/CNT/N system with $L = 3$ is plotted in Fig. 1(a). The conductance peaks reflect the band structures of the finite-sized nanotubes, because the resonant states are close to the eigenvalues for small coupling Γ. In the π-electron tight-binding model, the defect-free nanotubes have complete electron-hole symmetry with their Fermi levels at zero.[7] Then the resonant states are symmetric around the Fermi energy $E_F = 0$. The Andreev reflection probability for the N/CNT/S system with $L = 3$ are plotted in Fig. 1(b). The resonant Andreev reflection reflects the distribution of the resonant states of the nanotube systems. Although the resonant peaks are similar to those in a normal N/CNT/N system, they are

different from the conventional resonant tunneling, because the conventional tunneling is completely forbidden for $|E| < \Delta$. In fact, these peaks come from the Andreev reflections. For the finite-sized pristine nanotubes, the resonant states are symmetric around the Fermi energy as mentioned above. Furthermore, the chemical potential of the right superconducting lead $\mu_R = 0$ is lined up with the Fermi energy of the nanotube. It is just located in the middle of two symmetric states with energy ϵ_i and $-\epsilon_i$. When the electron incident from the left lead has the energy ϵ_i corresponding the ith state of the nanotube, a hole can propagate back to the state with the energy $-\epsilon_i$. Then a Cooper pair creates in the right superconducting lead because of Andreev reflection. The conductance for the nanotube with $L = 4$ is plotted in Fig. 1(c). It is evident that both positions and heights of the resonant peaks depend on the nanotube length. There is one resonant peak with the amplitude of two units at the Fermi energy, which is absent for the nanotube with $L = 3$. Similarly, there is a resonant Andreev peak at the Fermi energy for the N/CNT/S system with $L = 4$ as shown in Fig. 1(d). This is attributed to the electronic properties of the nanotubes. The band structure of armchair nanotubes consists of two non-degenerate bands that cross the Fermi level at $k_F = 2\pi/3a$, with lattice constant a. Finite size effects in carbon nanotubes lead to the quantization of the energy levels. In general, one resonant peak appears at the Fermi energy with $L = 3N + 1$ (N denoting the number of carbon repeat units), because $k_F = 2\pi/3a$ is now an allowed wave vector, a large conductance exists due to a crossing of two resonant states at the Fermi energy.[23] For other lengths, k_F is not an allowed wave vector and no resonant state exists at the Fermi level, thus conductance is much smaller due to the energy gap between the resonant states. These are referred to as on-resonance and off-resonance of the Andreev reflection, respectively.

The impurity, such as the substitutional boron (nitrogen) and the vacancy, can greatly change the electronic structure of the nanotubes and then the transport properties. In general, the impurity increases the normal reflection.[10] The substitutional boron or nitrogen impurity in the infinite carbon nanotube lead to a quasibound state near the lower or upper subbands.[11] However, it is quite different for finite-sized carbon nanotubes. New resonant state appears when the incoming electron energies match those of the quasibound states induced by the impurity. The substitutional boron effects on the conductance of the N/CNT/N system with $L = 3$ are clearly shown in Fig. 2(a). Compared with Fig. 1(a), the impurity leads to one new peak below the Fermi energy. The resonant states for the

conduction and valence bands are quite different due to the impurity, because the electron-hole symmetry, present in perfect nanotubes within the π-band approximation, is broken.[8] The positions of the resonant peaks is not symmetric around the Fermi energy $E_F = 0$ due to the symmetry broken. The corresponding Andreev reflection probability is plotted in Fig. 2(b). It can be clearly seen the substitutional boron greatly reduces the Andreev reflection probability. Because of the broken of the electron-hole symmetry mentioned above, the energy levels of the finite-sized nanotubes are not symmetric around $E_F = 0$. Because the energy level ϵ_i does not have a corresponding one with $-\epsilon_i$, the condition for the Andreev reflection has been broken. When the electron incident from the left lead has the energy ϵ_i corresponding to the ith state, a hole can not propagate back to the state with the energy that is different from $-\epsilon_i$. The Andreev reflection is then reduced distinctly by the impurity. Fig. 2(c) shows the conductance for the nanotube with $L = 4$. It is seen that the original peak at the Fermi energy with the height of two units are splitted into two ones with the height of one unit each. One of the two peaks is still at the Fermi energy and the other one is above the Fermi level. The reason is that the single impurity breaks the mirror symmetry planes containing the tube axis, and then the two resonant states at the Fermi energy are now splitted into two ones. Fig. 2(d) shows the corresponding Andreev reflection probability for $L = 4$. The Andreev reflection for $L = 4$ is stronger than that for $L = 3$, because the resonant states are more symmetric for $L = 4$. Furthermore, there is also one peak at the Fermi energy due to the reasons mentioned above.

The conductance and the corresponding Andreev reflection probability for the nanotube with the substitutional nitrogen are plotted in Fig. 3. A substitutional nitrogen has similar effects on the conductance of the N/CNT/N system as the boron, but it induces one resonant state above the Fermi energy. The resonant state associated with boron or nitrogen is analogous to the acceptor or donor state in semiconductors.[11] The nitrogen impurity also reduces the Andreev reflection, because it breaks the symmetry of the resonant states of the finite-sized nanotubes. Because the electron-hole spectra becomes more symmetrical with stronger U, the degree of the symmetry broken is slighter. The reduction is not so heavily as that caused by the boron. Then the Andreev reflection becomes larger again for stronger U. Fig. 4 shows the effects of the vacancy on the conductance and the Andreev reflection. For the very large U, as shown in Fig. 4(a), the resonant states become symmetric again. However, it is quite different from Fig. 1(a). One new peak emerges near the Fermi energy,

which is quite different from that of the perfect nanotubes. The position of the resonant state caused by the impurity approaches to the Fermi energy for a very strong U.[10] Then, it is expected that the vacancy dose not reduce the Andreev reflection, which can be seen from Fig. 4(b). For the off-resonant nanotube, the vacancy causes the appearance of a resonance state at the Fermi energy, where it is originally zero for the perfect nanotube. For the on-resonant nanotube, the vacancy induces a new resonant peak at the Fermi energy as shown in Fig. 4(c). The original one at the Fermi energy is splitted into two smaller ones around the Fermi energy. Because the electron-hole symmetry is recovered, the Andreev reflection becomes stronger again as shown in Fig. 4(d).

The Andreev reflection current versus the gate voltage is also investigated at different bias. As shown in Fig. 5(a)-(c), the current for the nanotube with $L = 3$ exhibits a single series of peaks with different spacings at very small bias, which reflects the band structure of the finite-sized nanotubes with the substitutional impurity. At a larger bias, as shown in Fig. 5(d)-(e), a series of extra peaks emerges. And they are located in the middle of the original ones at the low bias. Furthermore, the amplitude of some original peaks become larger and reaches a height three times its value at the low bias. The reason is that more energy levels contribute to the Andreev reflection at high bias. When $V > \Delta\epsilon/2$, a series of extra peaks can emerge between the original ones. And when $V > \Delta\epsilon$, the height of the original peaks can become about three times the original value.[20] Due to the different energy spacings, for some high bias, both of the conditions mentioned above can be satisfied. The impurity effects on the Andreev reflection current for the tube with $L = 4$ are clearly shown in Fig. 6. There are more peaks in the current at the same bias compared with Fig. 5. For nanotube with longer length, the spacing between energy levels become smaller. Because more resonant states contribute to the current at the same bias, there are more peaks in the Andreev reflection current. The complicated resonance patterns with different kinds of peaks depend on the bias, the level spacing of the CNT. It is also found that the exact location of the impurity has less influence on this significant feature than the strength of the impurity.

In summary, the probability and the current of the Andreev reflection for the N/CNT/S hybrid system are studied in detail. The Andreev reflection exhibits the on-resonance and off-resonance behavior at the Fermi energy for the nanotubes with $L = 3N + 1$ and other lengths, respectively. The substitutional boron, nitrogen and vacancy are simulated by

different impurity strength U. The substitutional boron or nitrogen breaks the electron-hole symmetry of the nanotube and reduces the Andreev reflection greatly. The symmetry broken and the reduction depend on the impurity strength distinctly. The vacancy with very strong impurity strength does not reduce Andreev reflection, because it keeps the electron-hole symmetry. It can change the off-resonance to the on-resonance of the Andreev reflection at the Fermi energy. The Andreev reflection current shows a complicated behaviour at different bias, which reflect the complex band structure of the finite-sized nanotubes with the impurity.

[1] R. Saito, G. Dresselhaus, and M.S. Dresselhars, *Physical Properties of Carbon Nanotubes* (Imperial College Press, London, 1998).

[2] J.W. Mintmire, B.I. Dunlap, and C.T. White, Phys. Rev. Lett. **68**, 631 (1992).

[3] N. Hamada, S.I. Sawada, and A. Oshiyama, Phys. Rev. Lett. **68**, 1579 (1992).

[4] R. Saito, M. Fujita, G. Dresselhaus, and M.S. Dresselhars, Appl. Phys. Lett. **60**, 2204 (1992).

[5] M. Bochrath, W. Liang, D. Bozovic, J.H. Hafner,C.H. Lieber, M. Tinkham, and H. Park, Science **291**, 283 (2001).

[6] L. Chico, L.X. Benedict, S.G. Louie, and M.L. Cohen, Phys. Rev. B **54**, 2600 (1996).

[7] L. Chico, V.H. Crespi, L.X. Benedict, S.G. Louie, and M.L. Cohen, Phys. Rev. Lett. **76**, 971 (1996).

[8] L. Chico, M.P.L. Sancho, and M.C. Munoz, Phys. Rev. Lett. **81**, 1278 (1998).

[9] M.P. Anantram, and T.R. Govindan, Phys. Rev. B **58**, 4882 (1998).

[10] T. Kostyrko, M. Bartkowiak, and G.D. Mahan, Phys. Rev. B **59**, 3241 (1999); **60**, 10735 (1999).

[11] H.J. Choi, J. Ihm, S.G. Louie, and M.L. Cohen, Phys. Rev. Lett. **84**, 2917 (2000).

[12] K. Tsukagoshi, B.W. Alphenaar, and H. Ago, Nauure (London) **401**, 572 (1999).

[13] A. Yu. Kasumov, R. Deblock, M. Kociak, B. Reulet, H. Bouchiat, I.I. Khodos, Yu. B. Gorbatov, V.T. Volkov, C. Journet, and M. Burghard, Science **284**, 1508 (1999).

[14] A.F. Morpurgo, J. Kong, C.M. Marcus and H. Dai, Science **286**, 263 (1999).

[15] M.R. Graber, T. Nussbaumer, W. Belzig and C. Schonenberger, cond-mat/0403431, (2004).

[16] Y. Wei, J. Wang, H. Guo, H. Mehrez, and C. Roland, Phys. Rev. B **63**, 195412 (2001)

[17] J. Jiang, L. Yang, J. Dong, and D.Y. Xing, Phys. Rev. B **68**, 054519 (2003)

[18] A. L. Yeyati, A. Martin-Rodero, and J. C. Cruvas, Phys. Rev. B **54**, 7366 (1996),

[19] A. L. Yeyati, J. C. Cuevas, A. Lopee-Davalos, and Martin-Rodero, Phys. Rev. B **55**, R6137 (1999).

[20] Qing-feng Sun, Jian Wang, and Tsung-han Lin, Phys. Rev. B **59**, 3831 (1999).

[21] M. B. Nardelli, Phys. Rev. B **60**, 7828 (1999).

[22] M. B. Nardelli, and J. Bernholc, Phys. Rev. B **60**, 16338 (1999).

[23] D. Orlikowski, H. Mehrez, J. Taylor, H. Guo, J. Wang, and C. Roland, Phys. Rev. B **63**, 155412 (2001)

Figure Captions

Fig. 1. (a) and (b) are the conductance G and Andreev reflection probability T_A as a function of electron energy E for the N/CNT/N and N/CNT/S systems of $L = 3$, respectively. (c) and (d) are the corresponding G and T_A for the systems of $L = 4$, respectively.

Fig. 2. (a) and (b) are the conductance G and Andreev reflection probability T_A as a function of electron energy E for the N/CNT/N and N/CNT/S systems of $L = 3$ with a boron impurity, respectively. (c) and (d) are the corresponding G and T_A for the systems of $L = 4$, respectively.

Fig. 3. (a) and (b) are the conductance G and Andreev reflection probability T_A as a function of electron energy E for the N/CNT/N and N/CNT/S systems of $L = 3$ with a nitrogen impurity, respectively. (c) and (d) are the corresponding G and T_A for the systems of $L = 4$, respectively.

Fig. 4. (a) and (b) are the conductance G and Andreev reflection probability T_A as a function of electron energy E for the N/CNT/N and N/CNT/S systems of $L = 3$ with a vacancy, respectively. (c) and (d) are the corresponding G and T_A for the systems of $L = 4$, respectively.

Fig. 5. (a)-(c) are the Andreev reflection current I_A as a function of the gate voltage V_g at the bias $V = 0.03$ with a boron, a nitrogen, and a vacancy, respectively. (d)-(e) are the corresponding I_A at the bias $V = 0.3$. Here $L = 3$.

Fig. 6. (a)-(c) are the Andreev reflection current I_A as a function of the gate voltage V_g

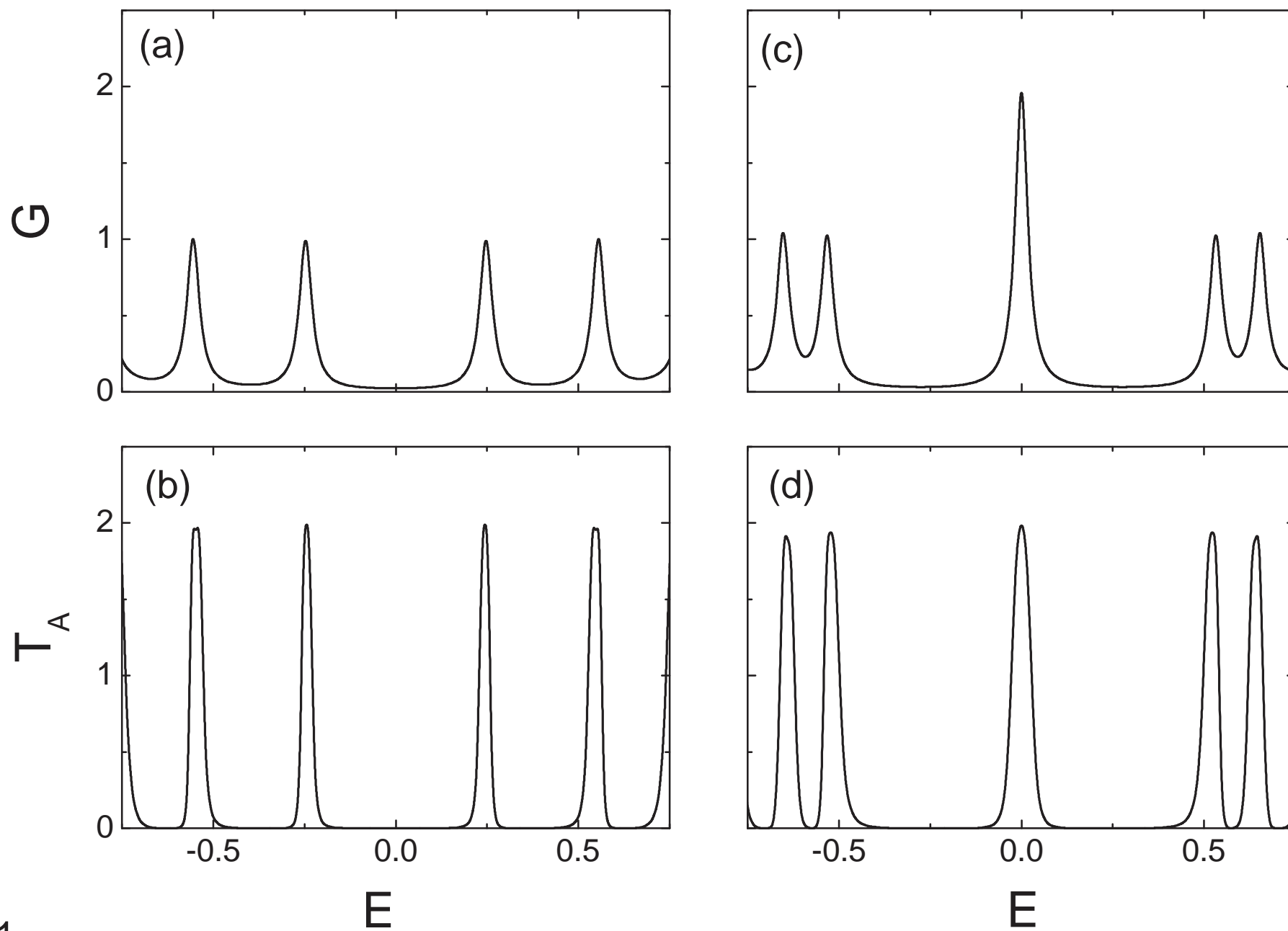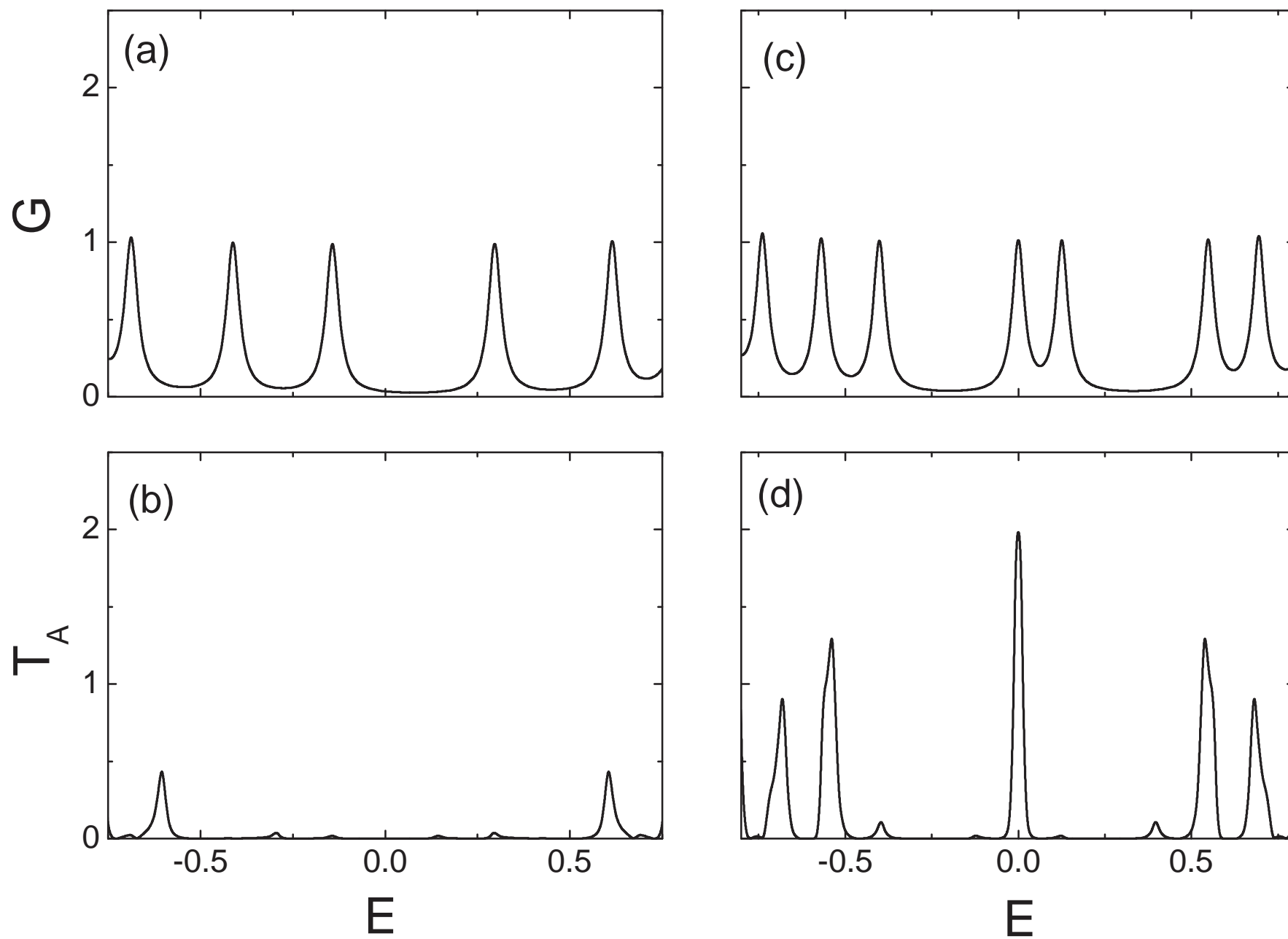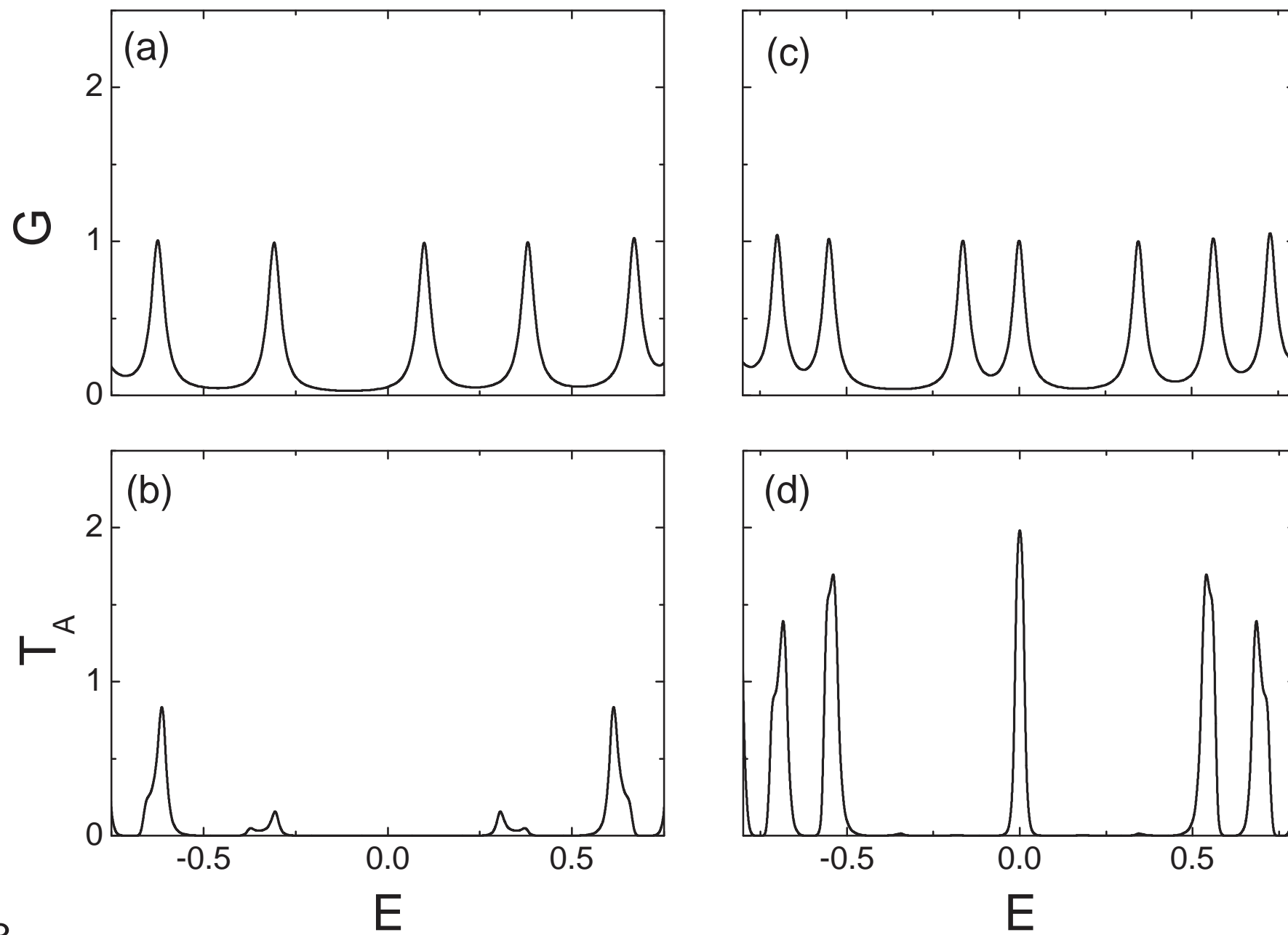at the bias $V = 0.03$ with a boron, a nitrogen, and a vacancy, respectively. (d)-(e) are the corresponding I_A at the bias $V = 0.3$. Here $L = 4$.
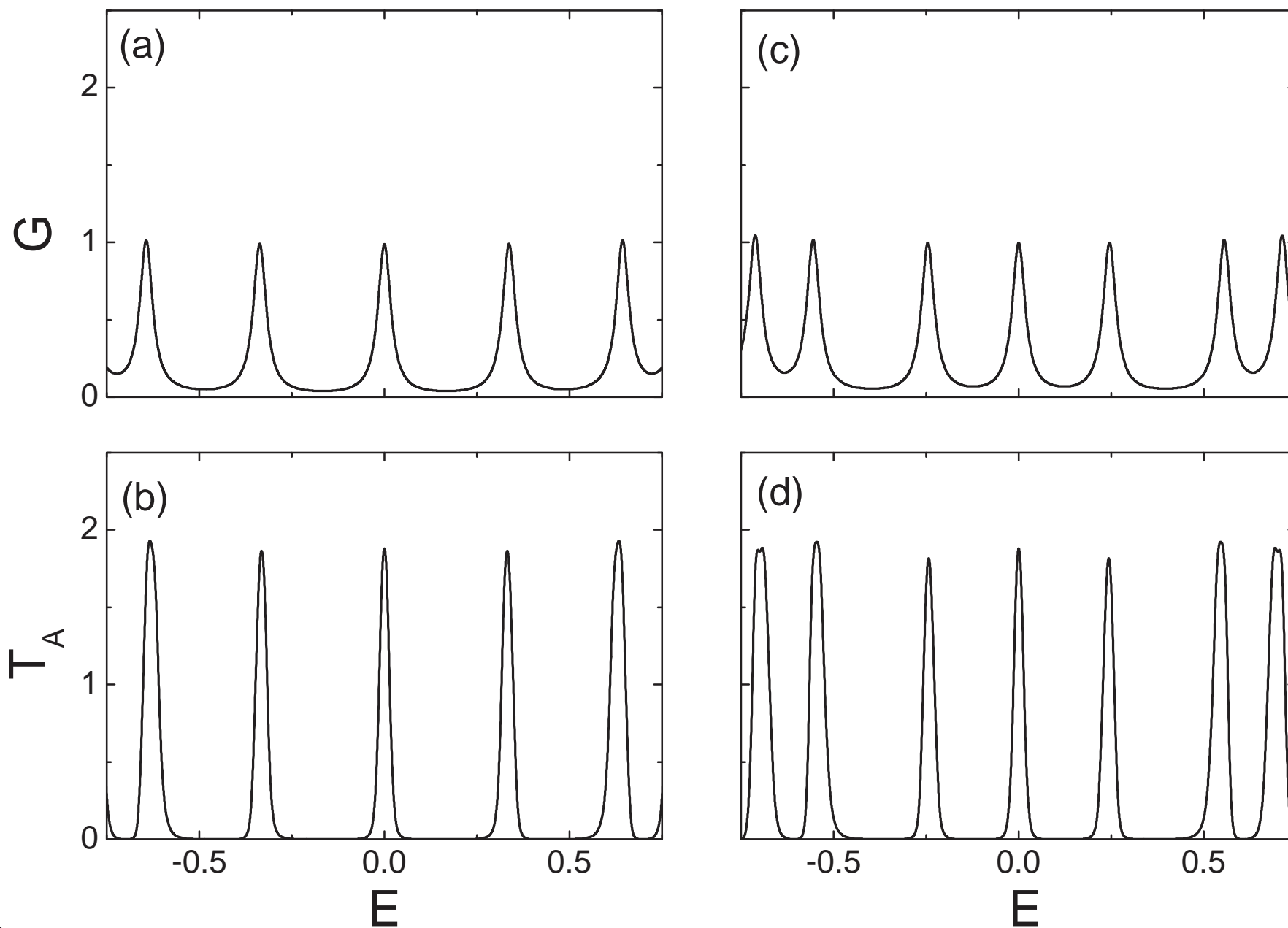
Fig. 1

Fig. 2

Fig. 3

Fig. 4

Fig. 5

Fig. 6